

Emergent continuous symmetry in anisotropic flexible two-dimensional materials

I. S. Burmistrov,^{1,2} V. Yu. Kachorovskii,³ M. J. Klug,⁴ and J. Schmalian^{4,5}

¹*L. D. Landau Institute for Theoretical Physics, Semanova 1-a, 142432, Chernogolovka, Russia*

²*Laboratory for Condensed Matter Physics, National Research University Higher School of Economics, 101000 Moscow, Russia*

³*A. F. Ioffe Physico-Technical Institute, 194021 St. Petersburg, Russia*

⁴*Institute for Theory of Condensed Matter, Karlsruhe Institute of Technology, 76131 Karlsruhe, Germany*

⁵*Institute for Quantum Materials and Technologies, Karlsruhe Institute of Technology, 76131 Karlsruhe, Germany*

We develop the theory of anomalous elasticity in two-dimensional flexible materials with orthorhombic crystal symmetry. Remarkably, in the universal region, where characteristic length scales are larger than the rather small Ginzburg scale ~ 10 nm, these materials possess an infinite set of flat phases which are connected by emergent continuous symmetry. This hidden symmetry leads to the formation of a stable line of fixed points corresponding to different phases. The same symmetry also enforces power law scaling with momentum of the anisotropic bending rigidity and Young's modulus, controlled by a single universal exponent – the very same along the whole line of fixed points. These anisotropic flat phases are uniquely labeled by the ratio of absolute Poisson's ratios. We apply our theory to monolayer black phosphorus (phosphorene).

The discovery of graphene [1–3] and closely related atomically thick materials [4] led to the field of flexible two-dimensional (2D) materials [5]. The hexagonal crystal symmetry of graphene results in elastic and electronic transport properties identical to those of isotropic system. More recently, research has shifted towards other 2D materials, including 2D black phosphorus (phosphorene) [6, 7], transition metal dichalcogenide monolayers [8, 9], and metal monochalcogenide monolayers [10, 11]. Because of their different crystal structure, these 2D materials demonstrate anisotropic physical properties, such as electron and thermal transport, optical absorption, photoluminescence, Raman scattering, and – as will be important in this paper – elastic response. In particular, for 2D materials with orthorhombic crystal symmetry, e.g. phosphorene, metal monochalcogenide monolayers (SiS, SiSe, GeS, GeSe, SnS, SnSe), monolayers GeAs₂, WTe₂, ZrTe₅, Ta₂NiS₅, etc. [12], the elastic free energy *does not* reduce to that of an isotropic crystalline membrane and results in anisotropic Young's moduli and Poisson's ratios.

The idea of anomalous elasticity of isotropic crystalline membranes dates back to the seminal work by Nelson and Peliti [13]. Later it was found that the competition between anomalous elasticity and thermal fluctuations in clean membranes leads to the existence of a transition from a flat to a crumpled phase with increasing of temperature [14–19]. Currently there is substantial interest in furthering our understanding of clean crystalline membranes [20–29].

In this Letter we develop the theory of anomalous elasticity of 2D membranes with orthorhombic crystal symmetry. Our theory is focused on the universal regime when the typical size, L , of the membrane is large in comparison with the so-called Ginzburg scale, q_*^{-1} . As we show, for the mentioned 2D materials $q_*^{-1} \sim 10$ nm is extremely small, making the universal regime experimentally highly relevant. We predict that for $L \gg q_*^{-1}$,

in contrast to graphene and dichalcogenide monolayers, these 2D materials possess an *infinite set* of flat phases with universal size-dependent anisotropic elastic properties. Although these phases perfectly preserve the orthorhombic anisotropy, they are connected by an emergent continuous symmetry. The latter ensures that the anisotropic anomalous Hooke's law is controlled by the same universal exponent for all phases. Analyzing the effective interaction of soft flexural phonons, these results are obtained from renormalization group (RG) equations that govern scaling of the bending rigidity tensor $\varkappa_{\alpha\beta}$ with L . Here $\alpha, \beta \in \{x, y\}$ are spatial indices. We obtain a *line of stable fixed points* that describes an infinite set of anisotropic flat phases corresponding to different degrees of orthorhombicity $\varkappa_{xx}/\varkappa_{yy}$ (see Fig. 1). In all cases the angular-dependent bending rigidity, $\varkappa(\theta_{\mathbf{k}}) = \varkappa_{\alpha\beta}^{(0)} \hat{k}_\alpha^2 \hat{k}_\beta^2$, where $\hat{\mathbf{k}} = (\cos \theta_{\mathbf{k}}, \sin \theta_{\mathbf{k}})$ is the unit vector along the momentum \mathbf{k} , flows to an elliptic dependence on $\theta_{\mathbf{k}}$ controlled by the ratio $\gamma = (\varkappa_{xx}^{(0)}/\varkappa_{yy}^{(0)})^{1/4}$. The power law scaling with k is then governed by the uni-

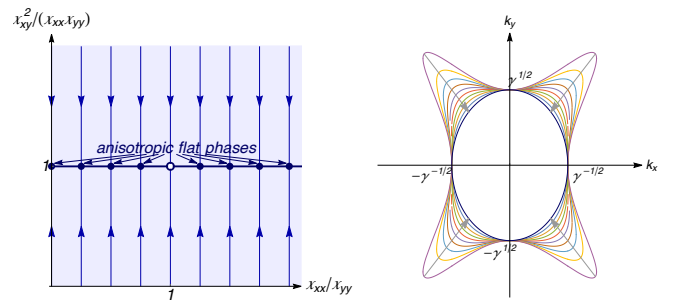


FIG. 1. Left: Sketch of the RG flow (arrows indicate direction of increase of a system size L). Anisotropic flat phases on the line of fixed points are marked by blue dots. The isotropic flat phase is indicated by the white point. Right: The contour plot of schematic change of the normalized bending rigidity $k^4 \varkappa(\theta_{\mathbf{k}}) / \sqrt{\varkappa_{xx} \varkappa_{yy}}$ under the RG flow for $\varkappa_{xx} > \varkappa_{yy}$, Eq. (9). For $\varkappa_{xx} < \varkappa_{yy}$ one needs to interchange the axes k_x and k_y .

versal exponent η (see Fig. 1 and Eqs. (9)). The emergent continuous symmetry ensures that η is the critical exponent for a flat isotropic membrane [30]. Finally, we study the transition to a tubular phase (discussed earlier in Refs.[31–35]), where an anisotropic 2D membrane is crumpled along one direction. We demonstrate that for a generic anisotropic membrane such transition occurs inevitably with increase of temperature. However, for the realistic above-mentioned 2D materials it happens at unphysically high temperature (of the order of tens of eV).

MODEL. — The free energy describing thermal fluctuations in the flat phase of a 2D membrane with orthorhombic crystal symmetry can be written as [31]

$$\mathcal{F} = \frac{1}{2} \int d^2 \mathbf{x} \left[\varkappa_{\alpha\beta}^{(0)} (\nabla_{\alpha}^2 \mathbf{r}) (\nabla_{\beta}^2 \mathbf{r}) + c_{11} u_{xx}^2 + c_{22} u_{yy}^2 + 2c_{12} u_{xx} u_{yy} + 4c_{66} u_{xy}^2 \right]. \quad (1)$$

Here, $u_{\alpha\beta} = (\partial_{\alpha} \mathbf{r} \partial_{\beta} \mathbf{r} - \delta_{\alpha\beta})/2$ where \mathbf{r} is a $d=d_c+2$ dimensional vector parametrizing the membrane. For physical membranes, $d_c=1$ while anharmonic effects can be efficiently described in terms of an expansion in $1/d_c$. The parameters $\{c_{\alpha\beta}, c_{66}\}$ denote the elastic moduli of 2D crystalline material. In the case of $\varkappa_{xx}^{(0)} = \varkappa_{yy}^{(0)}$ and $c_{11} = c_{22}$, the tetragonal crystal symmetry holds. For graphene which has the hexagonal symmetry, the bending energy is isotropic, $\varkappa_{xx}^{(0)} = \varkappa_{yy}^{(0)} = \varkappa_{xy}^{(0)}$ together with $c_{11} = c_{22} = \lambda + 2\mu$, $c_{12} = \lambda$, and $c_{66} = \mu$. For orthorhombic systems we allow for generic $c_{\alpha\beta}$ and c_{66} .

We choose the following parametrization of the coordinates: $r_1 = \xi_x x + u_x$, $r_2 = \xi_y y + u_y$, and $r_{a+2} = h_a$ with $a=1, \dots, d_c$, such that $u_{\alpha\beta} = (\xi_{\alpha}^2 - 1) \delta_{\alpha\beta} / 2 + \tilde{u}_{\alpha\beta}$, where

$$\tilde{u}_{\alpha\beta} = \frac{1}{2} \left(\xi_{\beta} \partial_{\alpha} u_{\beta} + \xi_{\alpha} \partial_{\beta} u_{\alpha} + \partial_{\alpha} \mathbf{h} \partial_{\beta} \mathbf{h} + \partial_{\alpha} \mathbf{u} \partial_{\beta} \mathbf{u} \right). \quad (2)$$

Here no summation over repeating indices is implied. The vectors $\mathbf{u} = \{u_x, u_y\}$ and $\mathbf{h} = \{h_1, \dots, h_{d_c}\}$ stand for in-plane and out-of-plane displacements, respectively. Assuming low enough temperatures (see below), we can neglect the term $\partial_{\alpha} \mathbf{u} \partial_{\beta} \mathbf{u}$ in comparison with $\partial_{\alpha} \mathbf{h} \partial_{\beta} \mathbf{h}$ in Eq. (2). Then, following Ref. [13], we integrate over \mathbf{u} and obtain the effective free energy written in terms of the out-of-plane phonons only [36],

$$\mathcal{F} = \frac{1}{8} \int d^2 \mathbf{x} c_{\alpha\beta} \varepsilon_{\alpha} \varepsilon_{\beta} + \frac{1}{2} \int \frac{d^2 \mathbf{k}}{(2\pi)^2} \varkappa_0(\theta_{\mathbf{k}}) k^4 \mathbf{h}_{\mathbf{k}} \mathbf{h}_{-\mathbf{k}} + \frac{1}{8} \int \frac{d^2 \mathbf{q}}{(2\pi)^2} Y_0(\theta_{\mathbf{q}}) \left| \int \frac{d^2 \mathbf{k}}{(2\pi)^2} \frac{[\mathbf{k} \times \mathbf{q}]^2}{q^2} \mathbf{h}_{\mathbf{k}+\mathbf{q}} \mathbf{h}_{-\mathbf{k}} \right|^2, \quad (3)$$

where we introduce $\varepsilon_{\alpha} = \xi_{\alpha}^2 - 1 + \int \frac{d^2 \mathbf{k}}{(2\pi)^2} k^2 \mathbf{h}_{\mathbf{k}} \mathbf{h}_{-\mathbf{k}}$. We assume that the following inequalities hold $\varkappa_{xx}^{(0)}, \varkappa_{yy}^{(0)} > 0$ and $\varkappa_{xy}^{(0)} > -(\varkappa_{xx}^{(0)} \varkappa_{yy}^{(0)})^{1/2}$. They guarantee that the bare angle-dependent bending rigidity $\varkappa_0(\theta) > 0$ for all angles

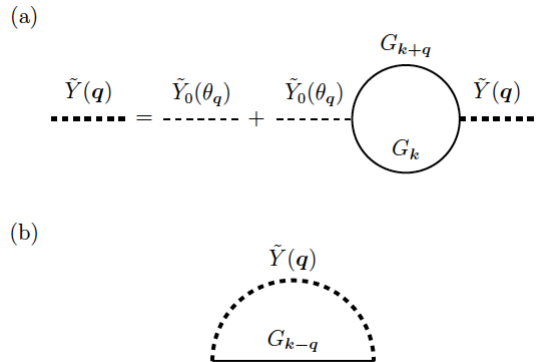


FIG. 2. (a) The RPA-type resummation for the Young's modulus. (b) The self-energy correction to first order in $1/d_c$. The solid line represents the bare Green's function $G_{\mathbf{k}}$. The thin (thick) dashed line denotes the (bare) screened interaction.

θ , such that the membrane is stable against transition into a tubular phase at zero temperature. The bare value of the Young modulus reads ($\varepsilon_{\alpha\beta}$ is fully antisymmetric tensor) [37]

$$Y_0(\theta_{\mathbf{q}}) = c_{66} \left[\hat{q}_x^2 \hat{q}_y^2 + \frac{c_{66} c_{\alpha\beta} \varepsilon_{\alpha\alpha'} \varepsilon_{\beta\beta'}}{c_{11} c_{22} - c_{12}^2} \hat{q}_{\alpha'}^2 \hat{q}_{\beta'}^2 \right]^{-1}. \quad (4)$$

The bending rigidity in Eq. (3) is subject to renormalization, $\varkappa_0(\theta) \rightarrow \varkappa(\theta)$, and, consequently, shows anomalous scaling. This can be fully described by the following running coupling constants,

$$\gamma = \left(\frac{\varkappa_{xx}}{\varkappa_{yy}} \right)^{1/4}, \quad \tilde{\varkappa} = (\varkappa_{xx} \varkappa_{yy})^{1/2}, \quad t = \frac{\tilde{\varkappa} - \varkappa_{xy}}{3\tilde{\varkappa} + \varkappa_{xy}}, \quad (5)$$

such that $0 < \gamma < \infty$ and $|t| < 1$. The parameter γ controls asymmetry between x and y axes existing in the orthorhombic symmetry class. The case $\gamma=1$ corresponds to the tetragonal symmetry, where t_0 describes the tetragonal distortion of the bending energy of the membrane. By rescaling of the momenta,

$$k_x \mapsto k_x / \sqrt{\gamma}, \quad k_y \mapsto k_y \sqrt{\gamma}. \quad (6)$$

one can represent the bending energy in Eq. (3) in a fashion formally similar to a system with the tetragonal symmetry,

$$\varkappa(\theta) \mapsto \tilde{\varkappa}(\theta) = \tilde{\varkappa} [1 + t \cos(4\theta)] / (1 + t). \quad (7)$$

We emphasize that after the rescaling (6) the free energy \mathcal{F} has still a symmetry that is lower than the tetragonal one due to the quartic term in h . The modified Young's modulus $\tilde{Y}_0(\theta)$ still depends explicitly on γ . However, the elastic properties of membranes in the universal region are independent of a particular form of $\tilde{Y}_0(\theta)$ [13, 14, 17].

RENORMALIZATION. — For $d_c \gg 1$ the effective free energy \mathcal{F} can be analyzed by treating the quartic interaction perturbatively. The necessary information can be extracted from the exact two-point Green's function $\langle h_i(\mathbf{k})h_j(-\mathbf{k}) \rangle \equiv \mathcal{G}_{\mathbf{k}}\delta_{ij}$ where the average is taken with respect to the free energy \mathcal{F} . The quadratic part of \mathcal{F} determines the bare Green's function $G_{\mathbf{k}} = T/[\tilde{\varkappa}_0(\theta_{\mathbf{k}})k^4]$.

As usual, the bare interaction, $\tilde{Y}_0(\theta)$, between flexural phonons is screened by RPA-type diagrams (see Fig. 2a). The screened interaction becomes independent of $\tilde{Y}_0(\theta)$ in the long wave limit, $q \ll q_*$ where $q_*^{-1} \sim [\varkappa_{xx}^{(0)}\varkappa_{yy}^{(0)}/(d_c\lambda T)]^{1/2}$, is the Ginzburg length. Here λ denotes a typical value of the elastic moduli. Therefore, at $q \ll q_*$ the theory (3) becomes independent of the coupling constant γ as a consequence of emergent hidden symmetry. The screened interaction behaves as q^2/d_c at $q \rightarrow 0$. This facilitates construction of the regular perturbation theory in $1/d_c$ for the self-energy $\Sigma_{\mathbf{k}} = G_{\mathbf{k}}^{-1} - \mathcal{G}_{\mathbf{k}}^{-1}$ (see diagram in Fig. 2b). The perturbation theory for $\Sigma_{\mathbf{k}}$ has infrared logarithmic divergences as $k \rightarrow 0$. They can be used to extract the RG behavior of the bending rigidity $\tilde{\varkappa}(\theta)$ (see Supplemental Material [38]).

The RG equations (to the lowest order in $1/d_c$) can be written in the following form ($\Lambda = \ln(q_*/k)$),

$$\frac{d\gamma}{d\Lambda} = 0, \quad \frac{dt}{d\Lambda} \simeq -\frac{2}{d_c}g(t), \quad \frac{d\ln\tilde{\varkappa}}{d\Lambda} \simeq \frac{2}{d_c}\chi(t), \quad (8)$$

where $t(0) = t_0$ and $\tilde{\varkappa}(0) = \tilde{\varkappa}_0$. We stress that the first of these equations is a consequence of the hidden symmetry and is not limited by $1/d_c$ expansion. We note also that $g(t)$ is an odd function. RG functions g and χ tend to constants as $t \rightarrow 1$ and have the following asymptotic expansions at $|t| \ll 1$: $g(t) \simeq (65t/54) + O(t^3)$ and $\chi(t) \simeq 1 - (65t/54) + (145t^2/162) + O(t^3)$ (see Fig. 3). For $t \rightarrow -1$ the function $g(t)$ tends to the constant whereas $\chi(t) \sim 1/(1+t)$. There exists an infra-red stable line of fixed points at $t=0$ at which the bending rigidity scales just like for isotropic membranes, $\tilde{\varkappa} \sim (q_*/k)^\eta$, where $\eta \simeq 2/d_c$. Eqs. (8) implies that the line of fixed points can only be reached asymptotically, $t \sim (k/q_*)^\psi$, with exponent $\psi \simeq 65/(27d_c)$. This crossover exponent determines the rate at which the bending rigidity approaches the elliptical form; see Fig. 1.

BEYOND $1/d_c$ EXPANSION. — The stable line of fixed points at $t=0$ emerges as the RG equations for t and $\tilde{\varkappa}$ in Eqs.(8) are independent of γ (see Fig. 1). We reiterate that the existence of the line of the fixed points is a direct consequence of the emergent hidden symmetry of the theory in the universal regime, $q \ll q_*$, and, thus, goes beyond the lowest order expansion in $1/d_c$. Hence, such line of fixed points exists for physical membranes with $d_c=1$. For arbitrary d_c (including $d_c=1$) it is natural to assume that (i) the line of stable fixed points remains stable ($\psi > 0$), (ii) there are no higher harmonics in $\tilde{\varkappa}(\theta)$ are generated under the RG flow, (iii) $t=0$ is the only fixed point in the interval $0 \leq t < 1$. Then, the elasticity of

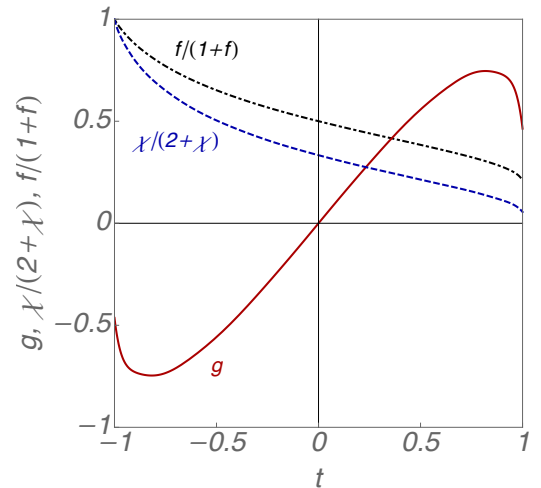


FIG. 3. The functions $g(t)$ and $\chi(t)$, that enter the RG Eqs. (8), and the function $f(t)$ that determines transition temperature to the tubular phase are shown.

2D membranes with the orthorhombic crystal symmetry in the universal regime can be deduced from anomalous elasticity of isotropic membranes.

Making inverse rescaling to Eq. (6), we find that in the original coordinate system the anomalous elasticity is described by the effective bending rigidity and Young's modulus:

$$\varkappa_{\text{eff}}(\mathbf{k}) \sim \left(\gamma \cos^2 \theta_{\mathbf{k}} + \gamma^{-1} \sin^2 \theta_{\mathbf{k}} \right)^{2-\eta/2} \left(\frac{q_*}{k} \right)^\eta, \quad (9)$$

$$Y_{\text{eff}}(\mathbf{q}) \sim \left[\left(\gamma \cos^2 \theta_{\mathbf{q}} + \gamma^{-1} \sin^2 \theta_{\mathbf{q}} \right)^{-1} \frac{q^2}{q_*^2} \right]^{1-\eta}.$$

At first glance, these equations obey only the discrete \mathbb{Z}_2 symmetry of orthorhombic phase, which is simply the discrete symmetry of an ellipse. Remarkably, there is also a hidden continuous symmetry related to the above mentioned rescaling. Indeed, after rescaling, the anisotropic problem with \varkappa_{xx} and \varkappa_{yy} is reduced to the isotropic one. The hidden symmetry is just an arbitrary rotation of this effective isotropic model.

The scaling of \varkappa_{eff} and Y_{eff} with the absolute value of momentum is controlled by the critical exponent η , known for the isotropic membrane. For $d_c \gg 1$ it is given as $\eta \simeq 2/d_c + (73 - 68\zeta(3))/(27d_c^2) + O(1/d_c^3)$ [26], whereas for $d_c=1$ the numerics predicts $\eta = 0.795 \pm 0.01$ [39]. The change of the angular dependence of the bending rigidity upon the RG flow is illustrated in Fig. 1. For $\gamma=1$, \varkappa_{eff} and Y_{eff} become independent of the angle. Thus a membrane with the tetragonal crystal symmetry is equivalent to an isotropic membrane in the universal regime.

The mechanics of a membrane on the line of the fixed points remains anisotropic. Under application of an unidirectional tension, σ_x , along the x axis the following deformations along the x and y axes are induced,

$$\delta\xi_x^2 \sim \gamma^{-1}(\sigma_x/\gamma)^\alpha, \quad \delta\xi_y^2 \sim \gamma(\sigma_x/\gamma)^\alpha. \quad (10)$$

Here the critical exponent α , which controls anomalous Hooke's law (10), is expressed via η exactly in the same way as in an isotropic membrane, $\alpha=\eta/(2-\eta)$. As expected, the membrane is deformed easier in the direction for which the bending rigidity is smaller. For example, from Eq. (10) it follows that $\delta\xi_y^2 > \delta\xi_x^2$ for $\gamma > 1$ ($\kappa_{xx}^{(0)} > \kappa_{yy}^{(0)}$). We note that the power-law behavior (10) holds for $\sigma_x \ll \sigma_* \sim \tilde{\kappa}_0 q_*^2$. The results for unidirectional tension along the y axis can be obtained from Eq. (10) under the following interchange $x \leftrightarrow y$ and $\gamma \leftrightarrow 1/\gamma$.

The anomalous Hooke's law (10) results in anisotropic *negative* absolute Poisson's ratio. In the anisotropic flat phase one finds for $\sigma_x, \sigma_y \ll \sigma_*$,

$$\nu_x = -\frac{\delta\xi_y^2(\sigma_x)}{\delta\xi_x^2(\sigma_x)} = \gamma^2 \nu, \quad \nu_y = -\frac{\delta\xi_x^2(\sigma_y)}{\delta\xi_y^2(\sigma_y)} = \frac{\nu}{\gamma^2}. \quad (11)$$

Here $\nu \approx -1 + 2/d_c - a/d_c^2 + O(1/d_c^3)$ with $a \approx 1.76 \pm 0.02$ denotes the absolute Poisson's ratio for the isotropic membrane [26]. We mention that the following relation holds, $\nu_x/\nu_y = \gamma^4$. Therefore, the measurement of the absolute Poisson's ratios in the regime of anomalous Hooke's law, $\sigma_x, \sigma_y \ll \sigma_*$, allows one to uniquely characterize the anisotropy in bending rigidity.

TUBULAR PHASE. — Usually, the crumpling transition is deduced from the equation of states that relates the stretching factor and the external tension. In the absence of the latter the equation of states, $\partial\langle\mathcal{F}\rangle/\partial\xi_\alpha^2 = \langle\varepsilon_\alpha\rangle = 0$, yields the dependence of ξ_α^2 on temperature. Instead, following Ref. [40], we introduce the momentum-dependent stretching factor, $\xi_\alpha^2(k) = 1 - d_c \int \frac{d^2q}{(2\pi)^2} \Theta(q-k) q_\alpha^2 \mathcal{G}_q$, that includes contributions from the flexural phonons with momenta q larger than a given momentum k . The dependence $\xi_x^2(k)$ can be cast in the form of the RG equation,

$$\frac{d\xi_x^2}{d\Lambda} = \frac{d_c T}{4\pi \kappa_{xx}^{3/4} \kappa_{yy}^{1/4}} \left(\frac{1+t}{1-t} \right)^{1/2}, \quad \xi_x^2(\Lambda=0) = 1. \quad (12)$$

The RG equation for ξ_y^2 can be obtained from Eq. (12) by interchange x and y . At low temperatures the flat phase, in which $\xi_\alpha^2(k)$ is positive for all $k < q_*$, is realized. For $\gamma < 1$, with increase of temperature $\xi_x^2(k)$ vanishes at some finite value of k . At the same time $\xi_y^2(k)$ is still positive for all $k < q_*$. Therefore, the tubular phase exists above the transition temperature $T_x = T_x^{(0)} f(t_0)$ where $T_x^{(0)} = (8\pi/d_c^2) [\kappa_{xx}^{(0)3} \kappa_{yy}^{(0)}]^{1/4}$ stands for the temperature of the crumpling transition at $t_0 = 0$. We note that the crumpling occurs along the direction, x , that corresponds to the smaller bare bending rigidity, $\kappa_{xx}^{(0)} < \kappa_{yy}^{(0)}$. The function $f(t)$ can be found from RG equations (8) and (12) [38]. We note that $f(t)$ is a monotonously decreasing function with $f(t \rightarrow -1) \sim (1+t)^{-1}$, $f(0) = 1$, and $f(1) \approx 0.3$. The function $f(t)$ is shown in Fig. 3. With even more increase of temperature the tubular phase experienced crumpled transition [32, 34]. For $\gamma < 1$ the tubular phase

at $T > T_y$ corresponds to $\xi_y^2(k=0) = 0$. The transition temperature T_y can be obtained from the expression for T_x upon interchange x and y .

DISCUSSION. — As illustration of our theory we employ it to 2D black phosphorus. We are not aware of direct measurements of elastic and bending moduli of phosphorene. Recent numerical calculations reports the following magnitudes: $c_{11} \approx 105.2$, $c_{22} \approx 26.2$, $c_{12} \approx 18.4$, and $c_{66} \approx 22.4$ (measured in N/m) [41] as well as $\kappa_{xx}^{(0)} \approx 8.0$ eV and $\kappa_{yy}^{(0)} \approx 4.8$ eV [42]. This yields the inverse Ginzburg length $q_* \approx 0.1$ nm⁻¹. Hence, anomalous elasticity should dominate elastic properties of available experimentally micron size samples. We remind that the Young's modulus and bending rigidity of graphene are 340 H/m and 1.4 eV, respectively, such that the inverse Ginzburg length at the room temperature is of the order 1 nm⁻¹. The anisotropy parameter can be estimated as $\gamma \approx 1.1$, indicating that the effective bending rigidity and Young's modulus, Eqs. (9), are expected to be slightly anisotropic.

For 2D black phosphorus our theory predicts that nonlinear Hooke's law, Eq. (10), and negative absolute Poisson's ratios, Eq. (11), should be observable for tensions smaller than $\sigma_* \approx 10^{-2}$ N/m. Although we are not aware of measurements of strain-stress dependence of phosphorene we believe that it can be performed in a way similar to graphene [43]. There are several computations of the Poisson's ratios for black phosphorus from first principles [44, 45]. While these results yield a negative Poisson's ratios of phosphorene, the numerical computation of the Poisson's ratio in the regime of low applied tensions, $\sigma_{x,y} \ll \sigma_*$, may suffer from a problem with proper boundary conditions in a finite size samples [25]. As in the case of graphene, a direct measurement of Poisson's ratio of phosphorene is challenging. We estimate the transition temperature to the tubular phase, $T_x^{(0)}$, to be of the order of 50 eV making anisotropic flat phase of phosphorene to be absolutely stable from the experimental point of view.

We also note that results (9) for the effective bending rigidity and Young's modulus are important for an electron transport in 2D materials. Recently, the anisotropy of the carrier mobility of 2D black phosphorus was studied using an effective bending rigidity of precisely the asymptotic form of Eq. (9) [46, 47].

It is worthwhile to mention that recently, distinct anisotropic model which breaks the $O(d)$ rotational invariance in the embedded space has been studied [48]. It would be interesting to study the effect of crystalline anisotropy discussed above in the model of Ref. [48].

To summarize, we developed the theory of anomalous elasticity in systems with orthorhombic crystal symmetry, relevant for a large number of recently studied 2D flexible materials. Our key finding is the hidden symmetry of the theory emerging in the universal regime that leads to existence of the infinite number of anisotropic

flat phases in the long-wave limit. These flat phases have anisotropic bending rigidity and Young's modulus whereas the scaling with momentum is the same as in the isotropic case. They are uniquely labeled by the ratio of absolute Poisson's ratios in the two perpendicular directions. Our theory can easily be extended to even less symmetric 2D materials with triclinic and monoclinic crystal symmetries, e.g. monolayers ReS_2 , ReSe_2 , GaTe , GeP , GeAs , SiP , SiAs , etc. Also, one can extend our theory to include the effects of in-plane and curvature disorder. The later was shown to be important for qualitative explanation of nonlinear strain-stress relation in graphene [49].

We thank M. Glazov and V. Lebedev for useful comments and discussions. The work was funded in part by the Alexander von Humboldt Foundation, by the Russian Ministry of Science and Higher Educations, the Basic Research Program of HSE, by the Russian Foundation for Basic Research, grant No. 20-52-12019, and by the Deutsche Forschungsgemeinschaft (DFG, German Research Foundation) project SCHM 1031/12-1.

-
- [1] K. S. Novoselov, A. K. Geim, S. V. Morozov, D. Jiang, Y. Zhang, S. V. Dubonos, I. V. Grigorieva, and A. A. Firsov, "Electric field effect in atomically thin carbon films," *Science* **306**, 666 (2004).
- [2] K. S. Novoselov, A. K. Geim, S. V. Morozov, D. Jiang, M. I. Katsnelson, I. V. Grigorieva, S. V. Dubonos, and A. A. Firsov, "Two-dimensional gas of massless dirac fermions in graphene," *Nature* **438**, 197 (2005).
- [3] Y. Zhang, Y.-W. Tan, H. L. Stormer, and P. Kim, "Experimental observation of the quantum hall effect and berry's phase in graphene," *Nature* **438**, 201 (2005).
- [4] K. S. Novoselov and A. H. Castro Neto, "Two-dimensional crystals-based heterostructures: materials with tailored properties," *Phys. Scr.* **T146**, 014006 (2012).
- [5] P. Avouris, T. F. Heinz, and T. Low, eds., "2D materials: Properties and devices," (Cambridge University Press, 2017).
- [6] X. Ling, H. Wang, S. Huang, F. Xia, and M.S. Dresselhaus, "The renaissance of black phosphorus," *PNAS* **112**, 4523 (2015).
- [7] M. Galluzzi, Y. Zhang, and X.-F. Yu, "Mechanical properties and applications of 2d black phosphorus," *J. Appl. Phys.* **128**, 230903 (2020).
- [8] G. Wang, A. Chernikov, M. M. Glazov, T. F. Heinz, X. Marie, Th. Amand, and B. Urbaszek, "Colloquium: Excitons in atomically thin transition metal dichalcogenides," *Rev. Mod. Phys.* **90**, 021001 (2018).
- [9] M. V. Durnev and M. M. Glazov, "Excitons and trions in two-dimensional semiconductors based on transition metal dichalcogenides," *Physics-Uspexhi* **61**, 825 (2018).
- [10] A. S. Sarkar and E. Stratakis, "Recent advances in 2D metal monochalcogenides," *Adv. Sci.* **7**, 2001655 (2020).
- [11] S. Barraza-Lopez, B. M. Fregoso, J. W. Villanova, S. S. P. Parkin, and K. Chang, "Colloquium: Physical properties of group-IV monochalcogenide monolayers," *Rev. Mod. Phys.* **93**, 011001 (2021).
- [12] L. Li, W. Han, L. Pi, P. Niu, J. Han, C. Wang, B. Su, H. Li, J. Xiong, Y. Bando, and T. Zhai, "Emerging in-plane anisotropic two-dimensional materials," *InfoMat.* **1**, 54 (2019).
- [13] D.R. Nelson and L. Peliti, "Fluctuations in membranes with crystalline and hexatic order," *J. Phys. (Paris)* **48**, 1085 (1987).
- [14] J. A. Aronovitz and T. C. Lubensky, "Fluctuations of solid membranes," *Phys. Rev. Lett.* **60**, 2634 (1988).
- [15] M. Paczuski, M. Kardar, and D. R. Nelson, "Landau theory of the crumpling transition," *Phys. Rev. Lett.* **60**, 2638 (1988).
- [16] F. David and E. Guitter, "Crumpling transition in elastic membranes: Renormalization group treatment," *Europhysics Lett. (EPL)* **5**, 709 (1988).
- [17] J. Aronovitz, L. Golubovic, and T. C. Lubensky, "Fluctuations and lower critical dimensions of crystalline membranes," *J. Phys. (Paris)* **50**, 609 (1989).
- [18] E. Guitter, F. David, S. Leibler, and L. Peliti, "Thermodynamical behavior of polymerized membranes," *J. Phys. (Paris)* **50**, 1787 (1989).
- [19] P. Le Doussal and L. Radzihovsky, "Self-consistent theory of polymerized membranes," *Phys. Rev. Lett.* **69**, 1209 (1992).
- [20] E. I. Kats and V. V. Lebedev, "Asymptotic freedom at zero temperature in free-standing crystalline membranes," *Phys. Rev. B* **89**, 125433 (2014).
- [21] E. I. Kats and V. V. Lebedev, "Erratum: Asymptotic freedom at zero temperature in free-standing crystalline membranes [Phys. Rev. B 89, 125433 (2014)]," *Phys. Rev. B* **89**, 079904 (2016).
- [22] I. S. Burmistrov, I. V. Gornyi, V. Yu. Kachorovskii, M. I. Katsnelson, and A. D. Mirlin, "Quantum elasticity of graphene: Thermal expansion coefficient and specific heat," *Phys. Rev. B* **94**, 195430 (2016).
- [23] A. Košmrlj and D. R. Nelson, "Statistical mechanics of thin spherical shells," *Phys. Rev. X* **7**, 011002 (2017).
- [24] I. S. Burmistrov, V. Yu. Kachorovskii, I. V. Gornyi, and A. D. Mirlin, "Differential Poisson's ratio of a crystalline two-dimensional membrane," *Ann. Phys. (N.Y.)* **396**, 119 (2018).
- [25] I. S. Burmistrov, I. V. Gornyi, V. Yu. Kachorovskii, M. I. Katsnelson, J. H. Los, and A. D. Mirlin, "Stress-controlled Poisson ratio of a crystalline membrane: Application to graphene," *Phys. Rev. B* **97**, 125402 (2018).
- [26] D.R. Saykin, I.V. Gornyi, V.Yu. Kachorovskii, and I.S. Burmistrov, "Absolute Poisson's ratio and the bending rigidity exponent of a crystalline two-dimensional membrane," *Ann. Phys. (N.Y.)* **414**, 168108 (2020).
- [27] O. Coquand, D. Mouhanna, and S. Teber, "The flat phase of polymerized membranes at two-loop order," *Phys. Rev. E* **101**, 062104 (2020).
- [28] A. Mauri and M. I. Katsnelson, "Scaling behavior of crystalline membranes: an ϵ -expansion approach," *Nucl. Phys. B* **956**, 115040 (2020).
- [29] A. Mauri and M. I. Katsnelson, "Scale without conformal invariance in membrane theory," *Nucl. Phys. B* **969**, 115482 (2021).
- [30] D. Nelson, T. Piran, and S. Weinberg, eds., *Statistical Mechanics of Membranes and Surfaces* (World Scientific, Singapore, 1989).
- [31] J. Toner, "Elastic anisotropies and long-ranged inter-

- actions in solid membranes,” *Phys. Rev. Lett.* **62**, 905 (1989).
- [32] L. Radzihovsky and J. Toner, “A new phase of tethered membranes: Tubules,” *Phys. Rev. Lett.* **75**, 4752 (1995).
- [33] M. Bowick, M. Falcioni, and G. Thorleifsson, “Numerical observation of a tubular phase in anisotropic membranes,” *Phys. Rev. Lett.* **79**, 885 (1997).
- [34] L. Radzihovsky and J. Toner, “Elasticity, shape fluctuations, and phase transitions in the new tubule phase of anisotropic tethered membranes,” *Phys. Rev. E* **57**, 1832 (1998).
- [35] K. Essafi, J.-P. Kownacki, and D. Mouhanna, “Crumpled-to-tubule transition in anisotropic polymerized membranes: Beyond the ϵ expansion,” *Phys. Rev. Lett.* **106**, 128102 (2011).
- [36] Here a ‘prime’ sign in the last integral indicates that the interaction with $q=0$ is excluded.
- [37] Q. Wei and X. Peng, “Superior mechanical flexibility of phosphorene and few-layer black phosphorus,” *Appl. Phys. Lett.* **104**, 251915 (2014).
- [38] Supplemental Material is available at.
- [39] A. Tröster, “Fourier monte carlo simulation of crystalline membranes in the flat phase,” *J. Phys.: Conf. Series* **454**, 012032 (2013).
- [40] I. V. Gornyi, V. Yu. Kachorovskii, and A. D. Mirlin, “Rippling and crumpling in disordered free-standing graphene,” *Phys. Rev. B* **92**, 155428 (2015).
- [41] L. Wang, A. Kutana, X. Zou, and B. I. Yakobson, “Electro-mechanical anisotropy of phosphorene,” *Nanoscale* **7**, 9746 (2015).
- [42] H.-Y. Zhang and J.-W. Jiang, “Elastic bending modulus for single-layer black phosphorus,” *J. Phys. D: Appl. Phys.* **48**, 455305 (2015).
- [43] R. J. T. Nicholl, H. J. Conley, N. V. Lavrik, I. Vlassiouk, Y. S. Puzyrev, V. P. Sreenivas, S. T. Pantelides, and K. I. Bolotin, “The effect of intrinsic crumpling on the mechanics of free-standing graphene,” *Nat. Commun.* **6**, 9789 (2015).
- [44] J.-W. Jiang and H. S. Park, “Negative poisson’s ratio in single-layer black phosphorus,” *Nat. Commun.* **5** (2014), 10.1038/ncomms5727.
- [45] Y. Du, J. Maassen, W. Wu, Z. Luo, X. Xu, and P. D. Ye, “Auxetic black phosphorus: A 2D material with negative Poisson’s ratio,” *Nano Lett.* **16**, 6701 (2016).
- [46] A. N. Rudenko, S. Brener, and M. I. Katsnelson, “Intrinsic charge carrier mobility in single-layer black phosphorus,” *Phys. Rev. Lett.* **116**, 246401 (2016).
- [47] S. Brener, A. N. Rudenko, and M. I. Katsnelson, “Effect of flexural phonons on the hole states in single-layer black phosphorus,” *Phys. Rev. B* **95**, 041406 (2017).
- [48] P. Le Doussal and L. Radzihovsky, “Thermal buckling transition of crystalline membranes in a field,” *Phys. Rev. Lett.* **127**, 015702 (2021).
- [49] I. V. Gornyi, V. Yu. Kachorovskii, and A. D. Mirlin, “Anomalous hooke’s law in disordered graphene,” *2D Materials* **4**, 011003 (2016).

ONLINE SUPPORTING INFORMATION

Emergent continuous symmetry in anisotropic flexible two-dimensional materials

I. S. Burmistrov,^{1,2} V. Yu. Kachorovskii,³ M. Klug,⁴ and J. Schmalian^{4,5}

¹*L. D. Landau Institute for Theoretical Physics, Semenov 1-a, 142432, Chernogolovka, Russia*

²*Laboratory for Condensed Matter Physics, National Research University Higher School of Economics, 101000 Moscow, Russia*

³*A. F. Ioffe Physico-Technical Institute, 194021 St. Petersburg, Russia*

⁴*Institute for Theory of Condensed Matter, Karlsruhe Institute of Technology, 76131 Karlsruhe, Germany*

⁵*Institute for Quantum Materials and Technologies, Karlsruhe Institute of Technology, 76131 Karlsruhe, Germany*

In this notes, we present (i) a derivation of the renormalization group equations to the lowest order in $1/d_c$ (Eq. 8 of the main text) and (ii) a derivation of the flat-to-tubule transition temperature.

S.I. RENORMALIZATION GROUP EQUATIONS TO THE LOWEST ORDER IN $1/d_c$

A. Effective interaction

Within RPA-type resummation scheme (see Fig. 2 of the main text) we obtain the screened interaction as

$$\tilde{Y}(\mathbf{q}) = \frac{\tilde{Y}_0(\theta_{\mathbf{q}})/2}{1 + 3\tilde{Y}_0(\theta_{\mathbf{q}})\Pi_{\mathbf{q}}/2}, \quad (\text{S1})$$

where the bare Young's modulus depends on the parameter γ ,

$$\tilde{Y}_0(\theta_{\mathbf{q}}) = 4\lambda_{xyxy} \left[\sin^2(2\theta) + 4\lambda_{xyxy} \frac{(\gamma^{-2}\lambda_{xxxx} \cos^4\theta - (\lambda_{xyxy}/2) \sin^2(2\theta) + \lambda_{yyyy}\gamma^2 \sin^4\theta)}{\lambda_{xxxx}\lambda_{yyyy} - \lambda_{xyxy}^2} \right]^{-1} \quad (\text{S2})$$

Here the polarization operator is given as

$$\Pi_{\mathbf{q}} = \frac{d_c}{3T} \int \frac{d^2\mathbf{k}}{(2\pi)^2} \frac{[\mathbf{k} \times \mathbf{q}]^4}{q^4} G_{\mathbf{k}+\mathbf{q}} G_{-\mathbf{k}} = \frac{d_c T}{q^2} \mathcal{P}(\theta_{\mathbf{q}}), \quad \mathcal{P}(\theta_{\mathbf{q}}) = \frac{1}{3} \int \frac{d^2\mathbf{k}}{(2\pi)^2} \frac{[\mathbf{k} \times \mathbf{q}]^4}{q^2} \frac{1}{(\mathbf{k} + \mathbf{q})^4 \tilde{\chi}_0(\theta_{\mathbf{k}+\mathbf{q}}) k^4 \tilde{\chi}_0(\theta_{-\mathbf{k}})}. \quad (\text{S3})$$

Such form of the screened interaction is justified to the lowest order in $1/d_c$. Similar to the isotropic case, in the long wave vector limit, $q \ll q_*$, the effective interaction of flexural phonons becomes

$$\tilde{Y}(\mathbf{q}) \rightarrow 1/(3\Pi_{\mathbf{q}}), \quad (\text{S4})$$

We note that in the absence of the anisotropy, $t_0=0$, the polarization operator is given as $\mathcal{P}(\theta_{\mathbf{q}})=1/(16\pi\tilde{\chi}_0^2)$.

B. Renormalization group equation

To the lowest order in $1/d_c$ the self-energy is given by diagram shown in Fig. 2 of the main text

$$\Sigma_{\mathbf{k}} = -\frac{2}{3}T \int \frac{d^2\mathbf{q}}{(2\pi)^2} \frac{[\mathbf{k} \times \mathbf{q}]^4}{q^4} \frac{G_{\mathbf{k}-\mathbf{q}}}{\Pi_{\mathbf{q}}} = -\frac{2}{3d_c} \int \frac{d^2\mathbf{q}}{(2\pi)^2} \frac{[\mathbf{k} \times \mathbf{q}]^4}{q^2} \frac{1}{|\mathbf{k} - \mathbf{q}|^4 \tilde{\chi}_0(\theta_{\mathbf{k}-\mathbf{q}}) \mathcal{P}(\theta_{\mathbf{q}})}. \quad (\text{S5})$$

The expression (S5) is logarithmically divergent. Within logarithmic accuracy at $k \ll q_*$, we obtain

$$\begin{aligned} \Sigma_{\mathbf{k}} \simeq & -\frac{1}{3\pi d_c} \left(k^4 \ln \frac{q_*}{k} \right) \int_0^{2\pi} \frac{d\theta_{\mathbf{q}}}{2\pi} \frac{\sin^4(\theta_{\mathbf{k}} - \theta_{\mathbf{q}})}{\tilde{\chi}_0(\theta_{\mathbf{k}-\mathbf{q}}) \mathcal{P}(\theta_{\mathbf{q}})} = -\frac{1}{24\pi d_c} \left(k^4 \ln \frac{q_*}{k} \right) \int_0^{2\pi} \frac{d\theta_{\mathbf{q}}}{2\pi} \frac{1}{\tilde{\chi}_0(\pi - \theta_{\mathbf{q}}) \mathcal{P}(\theta_{\mathbf{q}})} \\ & \times \left[3 - 4 \cos(2\theta_{\mathbf{k}}) \cos(2\theta_{\mathbf{q}}) + \cos(4\theta_{\mathbf{k}}) \cos(4\theta_{\mathbf{q}}) \right]. \end{aligned} \quad (\text{S6})$$

Here we used that $\theta_{\mathbf{k}-\mathbf{q}} \rightarrow \pi - \theta_{\mathbf{q}}$ as $k \rightarrow 0$.

It is convenient to introduce the dimensionless functions ($m=0, 1, 2$)

$$F_{2m}(t_0) = \frac{1}{16\pi} \int_0^{2\pi} \frac{d\theta}{2\pi} \frac{(1+t_0) \cos(2m\theta)}{\tilde{z}_0 \tilde{z}_0(\pi-\theta) \mathcal{P}(\theta)}. \quad (\text{S7})$$

We note that the normalization is such that $F_0(t_0=0)=1$ and $F_2(t_0=0)=F_4(t_0=0)=0$. Moreover, the symmetry of $\tilde{z}_0(\theta)$ implies that the function F_2 is zero identically, $F_2(t_0)\equiv 0$ whereas $F_0(t_0)$ ($F_4(t_0)$) is the even (odd) function of t_0 .

Converting perturbative result (S6) into the renormalization group equations, we find (see Eq. (8) in the main text)

$$\begin{aligned} \frac{dt}{d\Lambda} &= -\frac{2}{d_c} g(t), & g(t) &= tF_0(t) - F_4(t)/3, \\ \frac{d \ln \tilde{z}}{d\Lambda} &= \frac{2}{d_c} \chi(t), & \chi(t) &= \frac{F_0(t) + F_4(t)/3}{1+t}, \end{aligned} \quad (\text{S8})$$

where $\Lambda = \ln(q_*/k)$.

C. Asymptotic expressions for F_0 and F_4 for $0 \leq t < 1$

Performing integration in Eqs. (S3) and (S7), one finds the following asymptotic expressions at $t \ll 1$,

$$\mathcal{P}(\theta) \simeq \frac{(1+t)^2}{16\pi \tilde{z}_0^2} \left[1 + \frac{2}{9} \cos(4\theta)t + \frac{85 - 2 \cos(8\theta)}{90} t^2 + \frac{\cos(4\theta)(86 + 3 \cos(8\theta))}{315} t^3 + O(t^4) \right] \quad (\text{S9})$$

and

$$F_0(t) \simeq 1 - \frac{25}{81} t^2 + O(t^4), \quad F_4(t) \simeq -\frac{11}{18} t + \frac{527}{9720} t^3 + O(t^5). \quad (\text{S10})$$

Using the above results one can derive the asymptotic results for the functions $g(t)$ and $\chi(t)$ mentioned in the main text.

For $1-t \ll 1$, the integral over the angle $\theta_{\mathbf{k}}$ in Eq. (S3) is dominated by vicinity of $\pi/4$ and $5\pi/4$. At the same time the integral over absolute value of momentum is dominated by $k \sim q \sin(\theta_q + \pi/4)$. Then, evaluating the integral over \mathbf{k} in Eq. (S3), we find

$$\pi(\theta) \simeq \frac{1}{24} \frac{|\cos(2\theta)|}{1-t}, \quad |\theta - \pi/4| \gg \sqrt{1-t}. \quad (\text{S11})$$

In the limit $|\theta - \pi/4| \ll \sqrt{1-t}$, one can obtain that $\pi(\theta) \sim 1/\sqrt{1-t}$.

For $1-t \ll 1$ the integrals over θ in definitions of functions F_0 and F_4 , Eq. (S8), are dominated by the region $\theta \simeq \pi/4$. Hence, we find ($\theta = \pi/4 + \delta\theta$)

$$F_0(t) \simeq -F_4(t) \simeq \frac{24}{32\pi^2} \int_{\sqrt{1-t}}^{\infty} \frac{d(\delta\theta) (1-t)}{(1-t+8\delta\theta^2)|\delta\theta|} \sim \int_{\sim 1}^{\infty} \frac{d(\delta\theta)}{(1+8\delta\theta^2)|\delta\theta|} \quad (\text{S12})$$

Therefore, the functions $F_0(t)$ and $F_4(t)$ tend to a constant as $t \rightarrow 1$.

S.II. TRANSITION TO THE TUBULAR PHASE

Using (8) and (12) in the main text, we find

$$\xi_x^2(\Lambda) = 1 - \frac{T}{T_x^{(0)}} \int_t^{t_0} \frac{d\tau}{g(\tau)} \left(\frac{1+\tau}{1-\tau} \right)^{1/2} \exp \left(- \int_{\tau}^{t_0} du \frac{\chi(u)}{g(u)} \right) \quad (\text{S13})$$

where $T_x^{(0)} = (8\pi/d_c^2)[\mathcal{Z}_{xx}^{(0)3} \mathcal{Z}_{yy}^{(0)}]^{1/4}$. We note that Λ enters the right hand side of the above equation via $t \equiv t(\Lambda)$. For $T > T_x$, where

$$T_x = T_x^{(0)} f(t_0), \quad f(t_0) = \left[\int_0^{t_0} \frac{d\tau}{g(\tau)} \left(\frac{1+\tau}{1-\tau} \right)^{1/2} \exp \left(- \int_{\tau}^{t_0} du \frac{\chi(u)}{g(u)} \right) \right]^{-1} \quad (\text{S14})$$

the stretching factor ξ_x^2 vanishes at some finite value of Λ .

As one can check, the function $f(t_0)$ is monotonously decreasing function on the interval $-1 < t_0 < 1$. Using asymptotic results (S10), we find at $|t_0| \ll 1$,

$$f(t_0) \simeq 1 - t_0 + O(t_0^2). \quad (\text{S15})$$

For $t_0 \rightarrow 1$ the function $f(t_0)$ tends to a constant, whereas for $t_0 \rightarrow -1$ we obtain $f(t_0) \sim 1/(1+t_0)$.